Janus Membrane with Unparalleled Forward Osmosis Performance

Shenghua Zhou[a,b], Fu Liu*[a,b], Jianqiang Wang[a,b], Haibo Lin[a], Qiu Han[a], Shuaifei Zhao*[c] and Chuyang Y. Tang[d]

[a] Key Laboratory of Marine Materials and Related Technologies, Ningbo Institute of Materials Technology & Engineering, Chinese Academy of Sciences, No. 1219 Zhongguan West Rd, Ningbo, 315201, China

[b] University of Chinese Academy of Sciences, 19A Yuquan Rd, Shijingshan District, Beijing, 100049, China

[c] Department of Environmental Sciences, Macquarie University, Sydney, NSW 2109, Australia

[d] Department of Civil Engineering, The University of Hong Kong, Pokfulam Road, 999077, Hong Kong, S.A.R., PR China

*Corresponding authors:
Fu Liu
Tel.: +8657486325963
Fax: +8657486325963
E-mail: fu.liu@nimte.ac.cn

Shuaifei Zhao
Tel.: +61-2-98509672
Email: shuaifei.zhao@mq.edu.au

ABSTRACT

We report the use of highly porous Janus membranes with unparalleled forward osmosis (FO) performance in terms of water flux and reverse salt flux. A porous Janus FO membrane, comprised of a hydrophilic cellulose acetate layer and a hydrophobic polyvinylidene fluoride (PVDF) nanofiber layer, was fabricated by electrospinning. The resultant membrane exhibited outstanding FO performance, with a high water flux of 274.2 L m^{-2} h^{-1} and a low reverse salt flux of 1.65 g m^{-2} h^{-1} using 1 M NaCl draw solution. Different from the state-of-the-art thin film composite (TFC) membranes, the prepared Janus membrane demonstrates unparalleled FO performance via a nanofluidic diode model, whose high selectivity is determined by the air gap within the hydrophobic nanofiber layer that can effectively prevent the reverse salt diffusion. Wetting of the hydrophobic layer is the crucial issue in Janus FO membranes, which deserves further attention to extend the osmosis longevity.

INTRODUCTION

Forward osmosis (FO) is an emerging "engineered osmosis technology" for various desalination[1-3] and water treatment applications.[4-7] The driving force of FO is the osmotic pressure difference between a draw solution (DS) and a feed solution (FS), separated by a semi-permeable membrane. Considerable interests in FO are inspired by its nature of spontaneous diffusion, leading to low energy consumption.[8-10] However, FO still faces several challenges, such as membrane fouling,[11] internal concentration polarization (ICP)[12] and lack of high performance membranes.[13]

Developing high performance osmotic membranes has been a research focus in FO, as it can minimize both membrane fouling and ICP.[10, 14, 15] Desirable FO membranes should have high water permeability, ion selectivity and fouling resistance, but low structural parameter to mitigate ICP. Most high performance FO membranes consist of dense active layers and porous support layers. Numerous nanomaterials, such as graphene oxide,[16] carbon nanotubes,[13] aquaporins,[17] metal organic frameworks[18] and metals/metal oxides nanoparticles [19] have been incorporated either into the active layer or the support layer, or between these two layers. The traditional wisdom believes that both the support layer and the active layer are preferable to be highly hydrophilic to maximize membrane permeability[20-23] and minimize membrane fouling.[11, 15, 24, 25] More recently, a hydrophilic support-free selective layer was used for FO with zero ICP.[26] However, the mechanical stability and the difficult to scale up of the single-layer membrane prevent its wide spread applications.

Janus membranes with opposing properties at an interface have become emerging materials for various separations.[27] For the first time, we report a porous Janus membrane with outstanding forward osmosis performances. Such a Janus membrane is composed of a hydrophilic cellulose acetate (CA) layer and a hydrophobic polyvinylidene fluoride (PVDF) nanofiber layer via electrospinning (Figure 1a, b). The hydrophilic porous layer provides a mechanically stable low-fouling support to the hydrophobic layer. The air trapped in the hydrophobic layer offers a blocking barrier for reverse ions diffusion, leading to a high selectivity in FO. The unique air-gap structure could result in zero ICP on the hydrophobic side of the membrane, allowing for super high water permeability. The membrane surface and cross-sectional morphologies and surface hydrophilicity/hydrophobicity were evaluated. Both static diffusion and dynamic asymmetric transport behaviors of the Janus FO membrane were investigated. Forward water flux and reverse salt flux of the Janus membrane were tested and compared with the performances of the state-of-the-art FO membranes. The recovery of FO performance was evaluated by simply drying the membrane. This work provides a new Janus membrane with unparalleled FO performance via a nanofluidic diode model as depicted in Figure 1b.

MATERIALS AND METHODS

Materials. PVDF polymer (average M_w = 180,000) from Sigma-Aldrich (France) was dried at 80 °C for 24 h before preparing the membrane. N, N-Dimethylformamide (DMF), sodium chloride (NaCl) and methylene blue were purchased from Sinopharm

Chemical Reagent Co., Ltd, China and used without further purification. Hydrophilic cellulose acetate membranes (average pore size: 2.0 μm; thickness: 90 μm) were supplied by Haiyan New Oriental Plastic Technology Co., Ltd. Deionized (DI) water was employed to prepare the solutions.

Fabrication of Janus membrane. 12.5 g PVDF was dissolved in 37.5 g DMF at 60 °C for 8 h with constant stirring to make a homogeneous solution. Janus membranes (M_J) were prepared by electrospinning PVDF layer on the support hydrophilic CA membrane (M_h) (Figure 1a).The support was mounted onto a rotating drum (diameter of 15 cm) to collect the electrosprayed PVDF nanofibers with a constant rolling rate of 90 rpm. The thickness of the hydrophobic PVDF layer was controlled by adjusting the spinning time (Figure 1c). The injection rate of the PVDF solution was maintained at 1.0 mL h^{-1} and the voltage applied to the needle was 15.5 kV. The fabricated Janus membrane composed of a hydrophilic CA layer and a hydrophobic PVDF layer, labeled as M_J, was then dried in vacuum at room temperature (~ 25 °C) for 5h for further evaluation.

Membrane Characterization. Field-emission scanning electron microscopy (FESEM, Hitachi S4800, Japan) was used to observe the morphologies of the hydrophilic CA membrane (M_h) and the Janus membrane (M_J). Water contact angles of the CA and PVDF layers of the Janus membranes were measured by a contact angle analyzer (DCAT21, Germany). The membrane porosity was calculated based on the mass measurements of the dry and wet samples using the following equation:

$$Porosity = \frac{\frac{m_w - m_d}{\rho_w}}{\frac{m_w - m_d}{\rho_w} + \frac{m_d}{\rho}} \times 100\% \quad (1)$$

where m_w and m_d are the weights (g) of wet and dry membranes, respectively, ρ_w (g cm^{-3}) and ρ (g cm^{-3}) are the densities of ethane diol (wetting solvent) and polymer, respectively.

Membrane Performance Test. A lab-scale diffusion cell (Figure S1) was used to measure the diffusion of salt across M_h and M_J. The membrane was fixed between two chambers. One chamber was filled with DI water (35 mL) and the other one was filled with 1 M NaCl draw solution (35 mL). The rate of salt diffusion over time was determined based on the conductivity change of DI water, monitored by conductivity meter (CON2700, Eutech, USA).

Janus membrane performance in terms of water flux and reverse salt flux was tested by a lab-scale cross-flow FO membrane system at 25 ± 0.5 °C (Figure S2). A customized FO membrane cell with two symmetric flow channels (the radius of the membrane was 1.5 cm) was used and its effective area is 7.1 cm^2. The cross-flow rate was 0.3 L min^{-1} for the feed and draw solutions, controlled by peristaltic pumps (Masterflex, Cole-Parmer). In our study, DI water was used as the feed solution (FS) and NaCl solution with different concentration (0.2, 0.5, 1.0, 1.5 and 2.0 M) were used as the draw solution (DS). FO water flux (*Jw*) across the membrane was calculated based on the weight increase of the DS with a precision balance (Metler-Toledo) by Equation S1. The reverse salt flux, *Js*, was determined based on the NaCl concentration

in the feed solution by Equation S2, which was continuously monitored with the conductivity meter.

RESULTS AND DISCUSSION

Membrane Fabrication

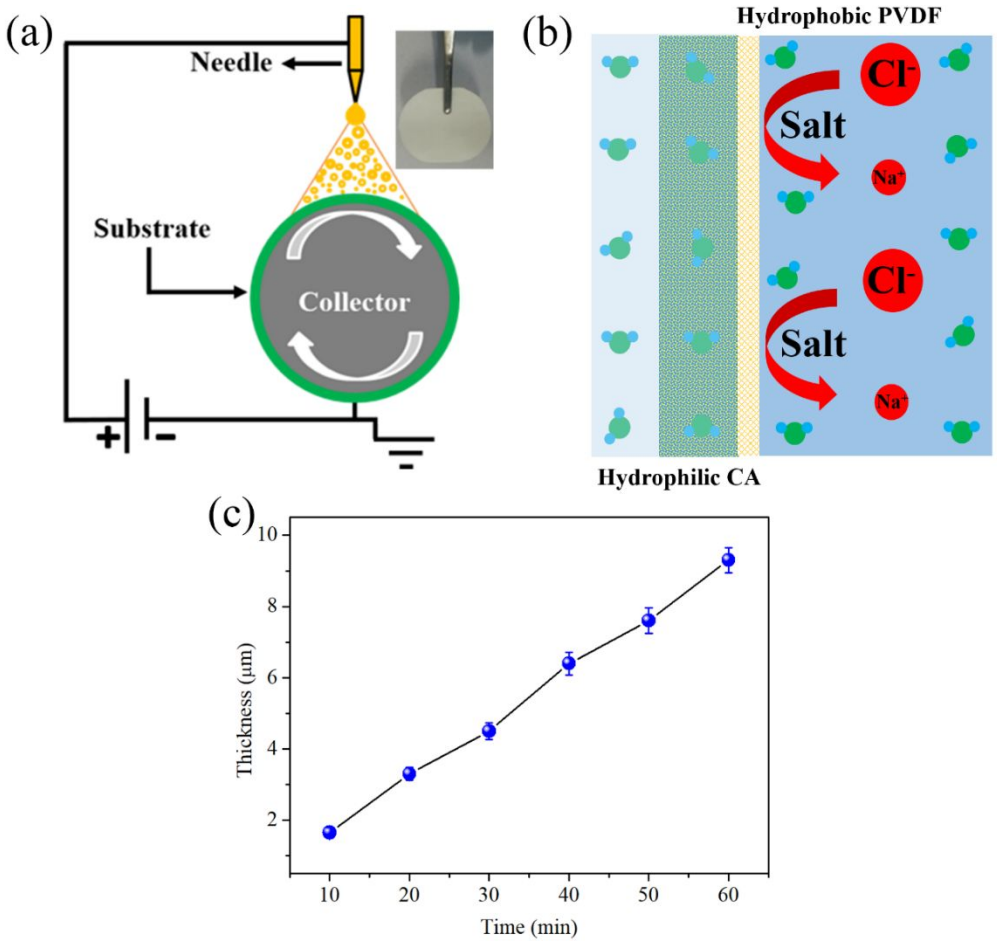

Figure 1. (a) Electrospinning for fabricating the Janus membrane, the inset is the photo of the prepared Janus membrane; (b) The unidirectional transport of water and salt ions repulsion through the Janus membrane containing an air gap via a nanofluidic diode model; (c) The thickness of the PVDF layer increased linearly with the electrospray time.

We prepared the Janus membrane by electrospinning hydrophobic PVDF nanofibers onto a hydrophilic CA layer. In our study, there was no pretreatment for the CA layer.

In the future, the CA layer can be pretreated by adhesives, such as polydopamine to enhance the long-term stability between the CA layer and the PVDF layer. The thickness of the hydrophobic PVDF layer varied from 1.7 to 9.1 μm by adjusting the spinning time (Figure 1c). The trapped air in the hydrophobic PVDF layer with micro-scale thickness offers a free pathway for water molecules transport through the membrane with low resistance, different from the high resistance mass transfer through the dense active layer of conventional TFC FO membranes with nano-scale thickness (typically a few tens to hundreds of nm).[28-30]

Dynamic cross-flow tests demonstrate that the fabricated Janus membrane has unidirectional transport of water. Namely, water preferentially transports from the hydrophilic side to the hydrophobic side, while salt ions in the draw solution are well isolated by the hydrophobic layer containing an air gap (Figure 1b). The hydrophobicity of vapor gap membranes leads to the formation of an air gap between the draw and feed streams. In contrast, with the hydrophobic layer facing to the feed solution, the Janus membrane shows low water flux and low rejection to salt. The static diffusion and dynamic cross-flow tests further confirmed the extremely high rejection of reverse salt diffusion by the Janus membrane, compared to the massive salt diffusion through the hydrophilic CA membrane in the absence of hydrophobic layer (Figures S3, S4). Because of the presence of the air gap, salt ions from the draw solution cannot enter the porous structure of the Janus membrane. The directional transport behavior of water

and salt through the Janus membrane is analogous to a nanofluidic diode in which water transport is favoured in one direction but supressed in the opposite direction.[31]

Membrane Characterization

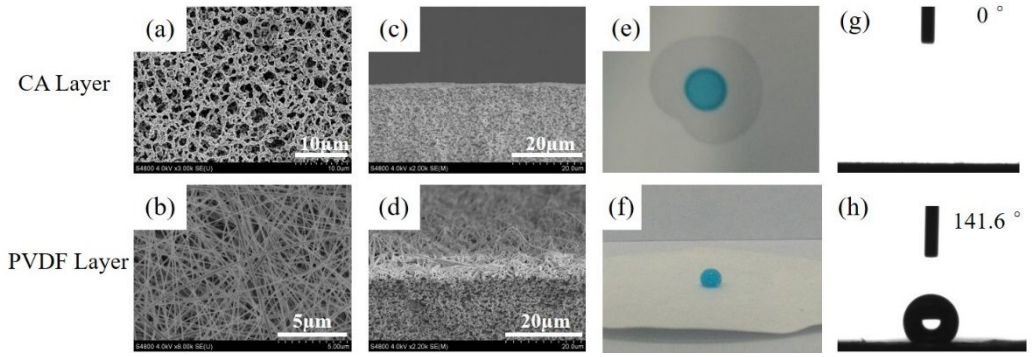

Figure 2. (a, b) Surface morphologies and (c, d) cross-sectional images of CA and PVDF layer of the Janus membrane; (e, f) water droplets on and (g, h) water contact angles of both sides of the Janus membrane, showing opposite wetting and anti-wetting behavior. The PVDF layer with a thickness of 3.3 μm was used for characterization.

The CA support layer (thickness 90 μm) and the PVDF thin layer (thickness 3.3 μm) of the Janus membrane were characterized by SEM and water contact angle measurement (Figure 2). The support CA membrane has typical spongy-like pores formed by phase inversion (Figure 2a). After electrospinning of PVDF, numerous nanofibers covered on the CA support to form an intertwined nanofiber layer with decreased pore size (Figure 2b, d, S5). The thickness of this hydrophobic PVDF layer, which plays the critical roles in trapping air and preventing ion transfer, can be precisely controlled by simply adjusting the electrospinning time (Figure 1c).

Water contact angle measurement confirms that the CA support membrane is highly hydrophilic, with a water contact angle of nearly 0° (Figure 2e, g). The hydrophilic CA

layer is anticipated to protect the hydrophobic layer and allow it to be resistant to flow shearing and fouling. By guiding the water flow through the porous CA structure, the air trapped in the hydrophobic PVDF layer (water contact angle = 141.6 ± 1°, salt water contact angle is 140 ± 2°, Figure 2f, h) with high wetting potential (7500 Pa, Figure S6) is better kept from being flushed away.

Separation Performance

To better understand the transport behavior of Janus membrane, the influence of the hydrophobic layer thickness on water and reverse salt flux was investigated. Both the water flux and reverse salt flux of the Janus membrane decrease with increasing the thickness of the hydrophobic PVDF layer or decreasing the osmotic pressure, corresponding to the draw solution concentration (Figure 3a, b). Our porous Janus membrane displays unparalleled water flux and reverse salt selectivity. For example, the Janus membrane with a PVDF layer thickness of 1.7 μm shows ultra-high water flux up to 274.2 L m^{-2} h^{-1} and low reverse salt flux of 1.65 g m^{-2} h^{-1} under typical conditions (DI water as FS, 1 M NaCl as DS at room temperature). The corresponding specific reverse salt flux (*Js/Jw*) was extremely low (0.006 g L^{-1}). Our water flux is almost four times higher than the so far highest flux recorded in literature (70 L m^{-2} h^{-1} with the selective layer against the feed).[22] The super high water flux is closely related to the high porosity (91.2%) of the PVDF layer of the membrane, compared to previous nanofluidic transport via alumina membrane (porosity ~10%).[44] The reverse salt flux

of our membrane also keeps lowest. Such FO performance in terms of *Jw* and *Jw/Js* outperforms the results in the existing literature (Figure 3c).[17, 22, 32-40]

The super high water flux of the Janus membrane cannot be explained by the classical solution-diffusion model for FO.[41-43] The dense active layer of traditional TFC membrane presents a tremendous resistance to water transport, which limits the permeability of FO. In our study, the trapped air gap within the porous hydrophobic layer provides unidirectional nanofluidic diode-like channels for the ultra-fast water transport while rejecting the reverse salt diffusion. Here, we propose a diffusion-evaporation-condensation mechanism for the mass transfer of Janus membranes. Namely, before the hydrophobic layer was wetted, water molecules fast diffuse into the hydrophilic layer first, evaporate into vapor, go through the air gap in the hydrophobic layer, and then condensate on the liquid draw solution side. The osmotic pressure is to depress the vapour pressure on the draw solution side, therefore driving the diode-like vapour transport across the hydrophobic PVDF layer. In addition, the hydrophobic PVDF side is able to block the ion reverse diffusion due to the presence of air gap layer. Similar phenomena were reported in nanofluidic applications[44] and osmotic distillation[45]. More systematic investigations on mass transfer mechanisms will be carried out in the future work. Indeed, the water flux and reverve salt flux increase almost linearly with the rise in DS concentration (Figure S7). Such performance is different from the rising trends in conventional FO, where water flux increases non-

linearly with the increase of the DS concentration (i.e. driving force) due to ICP.[12, 46] This suggests ICP in the porous hydrophobic layer can be negligible.

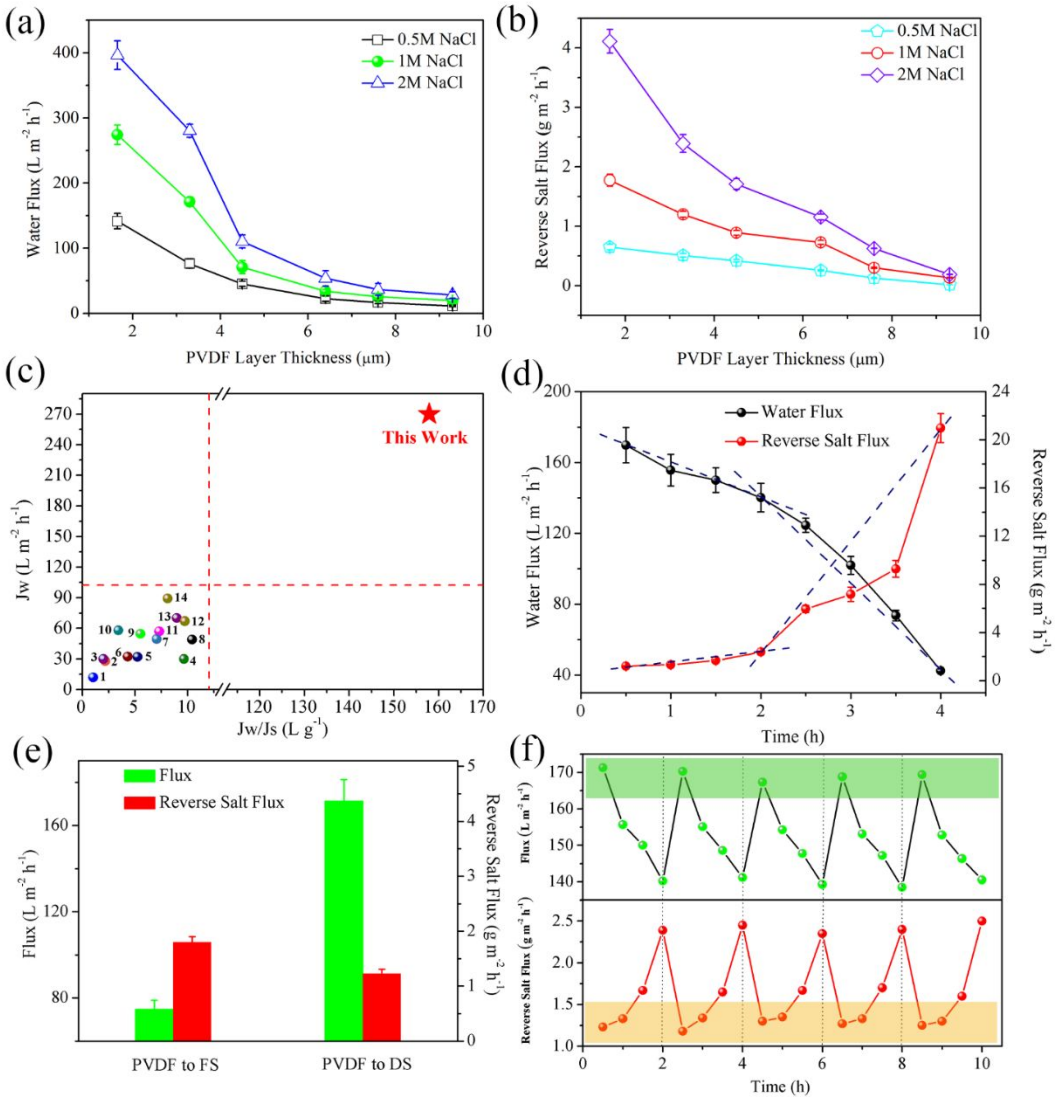

Figure 3. (a) Water flux and (b) reverse salt flux of the Janus membranes with varied PVDF layer thicknesses; DI water was used as feed solution and the PVDF layer faced the 1 M NaCl solution. (c) Osmosis performance of Janus membrane far outnumbers the-state-of-art FO membranes in literature. (d) Water flux and reverse salt flux as a function of operating time for the Janus membrane with a PVDF layer thickness of 3.3 μm; DI water was used as the feed solution and the PVDF layer faced 1 M NaCl solution. (e) Water flux and reverse salt flux of Janus membrane with the hydrophobic PVDF layer (thickness 3.3 μm) facing to the draw

solution (DS, 1M NaCl) and the feed solution (FS, DI water) respectively. (f) The recovery of water flux and reverse salt flux of the Janus membrane during 5 permeation-drying cycles; the PVDF layer thickness of the Janus membrane was 3.3 μm; DI water was used as the feed solution and the PVDF layer faced 1 M NaCl solution; natural drying was performed at room temperature for at least 10 h. All of these results were based on the crossflow FO tests.

Figure 3d shows the changes in water flux and reverse salt flux of the Janus membrane over time. Once the hydrophobic layer was partially wetted, salt could transport through the air-gap layer, and the FO performance was reduced accrodingly. Figure 3e compares the different FO water flux and reverse salt diffusion behavors in different operational modes. Obiviously, when the hydrophobic PVDF layer faces the draw solution, the Janus membrane shows a much higher water flux of 171.3 L m^{-2} h^{-1} but a lower reverse salt flux of 1.23 g m^{-2} h^{-1} than those in the other mode. Figure 3f shows the reversible FO separation performance of the Janus membrane. In the first 2 h, the drop in water flux was relatively small and the rise in reverse salt flux was also minimal, which is mainly caused by the dropping osmotic driving force as the DS is diluted without supplementing salts. After 2 h, the water flux and reverse salt flux show a significant inflection trend due to the severe wetting. However, we simply dried the Janus membrane after 2 h FO operation, both water flux and reverse salt flux nearly completely recovered in a 5-cycle test, indicating the essentiality of re-charged air in the hydrophobic PVDF layer.

IMPLICATIONS

In this study, we show a Janus membrane made of an electrospun hydrophobic PVDF layer supported by a hydrophilic CA layer. With the air gap trapped in the PVDF layer acting as nanofluidic diode-like channels, this Janus membrane exhibited ultra-fast water transport while rejecting the reverse salt diffusion in FO tests. The current study opens up a new avenue of developing porous Janus membranes with unprecedented osmosis performance. The porous Janus membranes with unparalleled osmosis performance may find their potential applications in desalination, juice and medicine concentration and power generation via pressure retarded osmosis.

Nevertheless, wetting plays an important role in the Janus membrane to deteriorate the membrane selectivity as well as FO water flux. Further research is therefore needed to enhance the anti-wetting performance of the Janus membrane in order to enable a long-term stable separation performance. The wetting resistance, fouling and scaling issue of the Janus membrane could be improved by reducing the pore size and porosity of the hydrophobic layer, or introducing a buffer layer between the hydrophobic layer and the DS (e.g. coating another hydrophilic layer on top of the hydrophobic layer) to minimize the impact of shearing force on wetting. In real application, it is possible to recover the performances by cleaning and drying once the membrane was fouled or wetted. Since membrane distillation which has the similar wetting issue has been commercialized, there is a good hope for our proposed Janus membrane for real application rather than only limited in lab. In addition, the long-term wetting resistance of the membrane can be enhanced by reducing the pores size or introducing protective layer (e.g. thin

hydrophilic layer or re-entrant structures with low surface energy via post-treatment, such as surface fluorination).[47-49] There should be a tradeoff between the membrane wetting resistance and porosity (flux). Our Janus membrane is structurally different from conventional TFC FO membrane. Systematic studies on the effect of the thickness and pore structure of each layer are thus needed to optimize the membrane separation performance and stability. Meanwhile, the typical parameters (e.g. structural parameter and ICP) and mass transfer mechanisms developed for conventional FO membranes/processes may not be directly applicable for Janus membranes. Thus, further studies are required to model the transport behavior for these novel FO membranes. We did not observe adhesion issues under the moderate experimental conditions, even though we did not performed any pretreatment for the CA layer. Where harsh operational conditions are applicable, the CA layer can be potentially pretreated by adhesives, such as polydopamine to enhance the long-term stability between CA layer and PVDF layer. In the future, Janus membranes with unique ionic transfer behaviors[50, 51] could significantly advance the osmotically driven membrane technology due to their superhigh FO performance demonstrated in this study.

ACKNOWLEDGEMENTS

Financial support is acknowledged from National Natural Science Foundation of China (51673209, 5161101025), Ningbo Science and Technology Bureau (2014B81004, 2017C110034). The authors also acknowledge the partial financial support from the

NSFC/RGC Joint Research Scheme sponsored by the Research Grants Council of Hong Kong and the National Natural Science Foundation of China (N_HKU706/16).

Supporting Information

The Supporting Information is available free of charge on the ACS Publications website at DOI: diagram of the diffusion cell (S1), diagram of the cross-flow FO system (S2), the salt diffusion across the membranes (S3), water permeability and reverse salt flux (S4) , the pore size distribution (S5), the wetting potential (S6), water flux and reverse salt flux as a function of draw solution concentration (S7).

Conflict of Interest

The authors declare no competing financial interest.

REFERENCES

1. Valladares Linares, R.; Li, Z.; Sarp, S.; Bucs, S. S.; Amy, G.; Vrouwenvelder, J. S., Forward Osmosis Niches in Seawater Desalination and Wastewater Reuse. *Water Research* **2014,** *66*, 122-139.

2. Zhao, S.; Zou, L.; Mulcahy, D., Brackish Water Desalination by A Hybrid Forward Osmosis-Nanofiltration System Using Divalent Draw Solute. *Desalination* **2012,** *284*, 175-181.

3. Qasim, M.; Darwish, N. A.; Sarp, S.; Hilal, N., Water Desalination by Forward (Direct) Osmosis Phenomenon: A Comprehensive Review. *Desalination* **2015,** *374*, 47-69.

4. Cath, T. Y.; Childress, A. E.; Elimelech, M., Forward Osmosis: Principles, Applications, and Recent Developments. *Journal of Membrane Science* **2006,** *281*, 70-87.

5. Zhao, S.; Zou, L.; Tang, C. Y.; Mulcahy, D., Recent Developments in Forward Osmosis: Opportunities and Challenges. *Journal of Membrane Science* **2012,** *396*, 1-21.

6. Shaffer, D. L.; Werber, J. R.; Jaramillo, H.; Lin, S.; Elimelech, M., Forward Osmosis: Where Are We Now? *Desalination* **2015,** *356*, 271-284.

7. Sukitpaneenit, P.; Chung, T. S., High Performance Thin-Film Composite Forward Osmosis Hollow Fiber Membranes with Macrovoid-Free and Highly Porous Structure for Sustainable Water Production. *Environmental Science & Technology* **2012,** *46*, (13), 7358-7365.

8. Long, Q.; Shen, L.; Chen, R.; Huang, J.; Xiong, S.; Wang, Y., Synthesis and Application of Organic Phosphonate Salts As Draw Solutes in Forward Osmosis for Oil-Water Separation. *Environmental Science & Technology* **2016,** *50*, (21), 12022-12029.

9. Chou, S.; Shi, L.; Wang, R.; Tang, C. Y.; Qiu, C.; Fane, A. G., Characteristics and Potential Applications of A Novel Forward Osmosis Hollow Fiber Membrane. *Desalination* **2010,** *261*, 365-372.

10. Qi, L.; Hu, Y.; Liu, Z.; An, X.; Bar-Zeev, E., Improved Anti-Biofouling Performance of Thin-Film Composite Forward-Osmosis Membranes Containing Passive and Active Moieties. *Environmental Science & Technology* **2018,** *52*, (17), 9684-9693.

11. She, Q.; Wang, R.; Fane, A. G.; Tang, C. Y., Membrane Fouling in Osmotically Driven Membrane Processes: A Review. *Journal of Membrane Science* **2016,** *499*, 201-233.

12. Zhao, S.; Zou, L., Relating Solution Physicochemical Properties to Internal Concentration Polarization in Forward Osmosis. *Journal of Membrane Science* **2011,** *379*, 459-467.

13. Zhou, Z.; Hu, Y.; Boo, C.; Liu, Z.; Li, J.; Deng, L.; An, X., High-Performance Thin-Film Composite Membrane with An Ultrathin Spray-Coated Carbon Nanotube Interlayer. *Environmental Science & Technology Letters* **2018,** *5*, (5), 243-248.

14. Suwaileh, W. A.; Johnson, D. J.; Sarp, S.; Hilal, N., Advances in Forward Osmosis Membranes: Altering the Sub-Layer Structure via Recent Fabrication and Chemical Modification Approaches. *Desalination* **2018,** *436*, 176-201.

15. Hegab, H. M.; ElMekawy, A.; Barclay, T. G.; Michelmore, A.; Zou, L.; Saint, C. P.; Ginic-Markovic, M., Single-Step Assembly of Multifunctional Poly(tannic acid)-Graphene Oxide Coating to Reduce Biofouling of Forward Osmosis Membranes. *ACS Applied Materials & Interfaces* **2016,** *8*, (27), 17519-17528.

16. Hegab, H. M.; ElMekawy, A.; Barclay, T. G.; Michelmore, A.; Zou, L.; Saint, C. P.; Ginic-Markovic, M., Fine-Tuning the Surface of Forward Osmosis Membranes via Grafting Graphene Oxide: Performance Patterns and Biofouling Propensity. *ACS Applied Materials & Interfaces* **2015,** *7*, (32), 18004-18016.

17. Li, X.; Loh, C. H.; Wang, R.; Widjajanti, W.; Torres, J., Fabrication of A Robust High-Performance FO Membrane by Optimizing Substrate Structure and Incorporating Aquaporin into Selective Layer. *Journal of Membrane Science* **2017,** *525*, 257-268.

18. Ma, D. C.; Peh, S. B.; Han, G.; Chen, S. B., Thin-Film Nanocomposite (TFN) Membranes Incorporated with Super-Hydrophilic Metal-Organic Framework (MOF) UiO-66: Toward Enhancement of Water Flux and Salt Rejection. *ACS Applied Materials & Interfaces* **2017,** *9*, (8), 7523-7534.

19. Soroush, A.; Ma, W.; Silvino, Y.; Rahaman, M. S., Surface Modification of Thin Film Composite Forward Osmosis Membrane by Silver-Decorated Graphene-Oxide Nanosheets. *Environmental Science: Nano* **2015,** *2*, 395-405.

20. Ma, D.; Peh, S. B.; Han, G.; Chen, S. B., Thin-Film Nanocomposite (TFN) Membranes Incorporated with Super-Hydrophilic Metal-Organic Framework (MOF) UiO-66: Toward Enhancement of Water Flux and Salt Rejection. *ACS Applied Materials & Interfaces* **2017,** *9*, (8), 7523-7534.

21. Li, Y.; Huang, S.; Zhou, S.; Fane, A. G.; Zhang, Y.; Zhao, S., Enhancing Water Permeability and Fouling Resistance of Polyvinylidene Fluoride Membranes with Carboxylated Nanodiamonds. *Journal of Membrane Science* **2018,** *556*, 154-163.

22. Liang, H. Q.; Hung, W. S.; Yu, H. H.; Hu, C. C.; Lee, K. R.; Lai, J. Y.; Xu, Z. K., Forward Osmosis Membranes with Unprecedented Water Flux. *Journal of Membrane Science* **2017,** *529*, 47-54.

23. Tiraferri, A.; Kang, Y.; Giannelis, E. P.; Elimelech, M., Highly Hydrophilic Thin-Film Composite Forward Osmosis Membranes Functionalized with Surface-Tailored Nanoparticles. *ACS Applied Materials & Interfaces* **2012,** *4*, (9), 5044-5053.

24. Shaffer, D. L.; Jaramillo, H.; Castrillon, S. R. V.; Lu, X.; Elimelech, M., Post-Fabrication Modification of Forward Osmosis Membranes with A Poly(ethylene glycol) Block Copolymer for Improved Organic Fouling Resistance. *Journal of Membrane Science* **2015,** *490*, 209-219.

25. Anh, N.; Zou, L.; Priest, C., Evaluating the Antifouling Effects of Silver Nanoparticles Regenerated by TiO2 on Forward Osmosis Membrane. *Journal of Membrane Science* **2014,** *454*, 264-271.

26. Li, M.; Karanikola, V.; Zhang, X.; Wang, L.; Elimelech, M., A Self-Standing, Support-Free Membrane for Forward Osmosis with No Internal Concentration Polarization. *Environmental Science & Technology Letters* **2018,** *5*, (5), 266-271.

27. Yang, H. C.; Hou, J.; Chen, V.; Xu, Z. K., Janus Membranes: Exploring Duality for Advanced Separation. *Angewandte Chemie International Edition* **2016,** *55*, (43), 13398-13407.

28. Yaroshchuk, A.; Bruening, M. L.; Licón Bernal, E. E., Solution-Diffusion-Electro-Migration Model and Its Uses for Analysis of Nanofiltration, Pressure-Retarded Osmosis and Forward Osmosis in Multi-Ionic Solutions. *Journal of Membrane Science* **2013,** *447*, 463-476.

29. Wang, J.; Dlamini, D. S.; Mishra, A. K.; Pendergast, M. T. M.; Wong, M. C. Y.; Mamba, B. B.; Freger, V.; Verliefde, A. R. D.; Hoek, E. M. V., A Critical Review of Transport through Osmotic Membranes. *Journal of Membrane Science* **2014,** *454*, 516-537.

30. Kong, F. X.; Yang, H. W.; Wu, Y. Q.; Wang, X. M.; Xie, Y. F., Rejection of Pharmaceuticals during Forward Osmosis and Prediction by Using the Solution-Diffusion Model. *Journal of Membrane Science* **2015,** *476*, 410-420.

31. Cheng, L. J.; Guo, L. J., Nanofluidic Diodes. *Chemical Society Reviews* **2010,** *39*, (3), 923-938.

32. Tian, M.; Qiu, C.; Liao, Y.; Chou, S.; Wang, R., Preparation of Polyamide Thin Film Composite Forward Osmosis Membranes Using Electrospun Polyvinylidene Fluoride (PVDF) Nanofibers As Substrates. *Separation and Purification Technology* **2013,** *118*, 727-736.

33. Han, G.; Zhao, B.; Fu, F.; Chung, T. S.; Weber, M.; Staudt, C.; Maletzko, C., High Performance Thin-Film Composite Membranes with Mesh-Reinforced Hydrophilic Sulfonated Polyphenylenesulfone (sPPSU) Substrates for Osmotically Driven Processes. *Journal of Membrane Science* **2016,** *502*, 84-93.

34. Stillman, D.; Krupp, L.; La, Y. H., Mesh-Reinforced Thin Film Composite Membranes for Forward Osmosis Applications: the Structure-Performance Relationship. *Journal of Membrane Science* **2014,** *468*, 308-316.

35. Cath, T. Y.; Elimelech, M.; McCutcheon, J. R.; McGinnis, R. L.; Achilli, A.; Anastasio, D.; Brady, A. R.; Childress, A. E.; Farr, I. V.; Hancock, N. T.; Lampi, J.; Nghiem, L. D.; Xie, M.; Yip, N. Y., Standard Methodology for Evaluating Membrane Performance in Osmotically Driven Membrane Processes. *Desalination* **2013,** *312*, 31-38.

36. Ong, R. C.; Chung, T. S.; de Wit, J. S.; Helmer, B. J., Novel Cellulose Ester Substrates for High Performance Flat-Sheet Thin-Film Composite (TFC) Forward Osmosis (FO) Membranes. *Journal of Membrane Science* **2015,** *473*, 63-71.

37. Liu, X.; Ng, H. Y., Double-Blade Casting Technique for Optimizing Substrate Membrane in Thin-Film Composite Forward Osmosis Membrane Fabrication. *Journal of Membrane Science* **2014,** *469*, 112-126.

38. Ren, J.; O'Grady, B.; deJesus, G.; McCutcheon, J. R., Sulfonated Polysulfone Supported High Performance Thin Film Composite Membranes for Forward Osmosis. *Polymer* **2016,** *103*, 486-497.

39. Zhao, Y.; Wang, X.; Ren, Y.; Pei, D., Mesh-Embedded Polysulfone/Sulfonated Polysulfone Supported Thin Film Composite Membranes for Forward Osmosis. *ACS Applied Materials & Interfaces* **2018,** *10*, (3), 2918-2928.

40. Ma, N.; Wei, J.; Qi, S.; Zhao, Y.; Gao, Y.; Tang, C. Y., Nanocomposite Substrates for Controlling Internal Concentration Polarization in Forward Osmosis Membranes. *Journal of Membrane Science* **2013,** *441*, 54-62.

41. Attarde, D.; Jain, M.; Chaudhary, K.; Gupta, S. K., Osmotically Driven Membrane Processes by Using A Spiral Wound Module-Modeling, Experimentation and Numerical Parameter Estimation. *Desalination* **2015,** *361*, 81-94.

42. Zhao, S., Osmotic Pressure versus Swelling Pressure: Comment on "Bifunctional Polymer Hydrogel Layers As Forward Osmosis Draw Agents for Continuous Production of Fresh Water Using Solar Energy". *Environmental Science & Technology* **2014,** *48*, (7), 4212-4213.

43. McCormick, P.; Pellegrino, J.; Mantovani, F.; Sarti, G., Water, Salt, and Ethanol Diffusion through Membranes for Water Recovery by Forward (Direct) Osmosis Processes. *Journal of Membrane Science* **2008,** *325*, 467-478.

44. Lee, J.; Laoui, T.; Karnik, R., Nanofluidic Transport Governed by the Liquid/Vapour Interface. *Nature Nanotechnology* **2014,** *9*, 317-323.

45. Lee, J.; Straub, A. P.; Elimelech, M., Vapor-Gap Membranes for Highly Selective Osmotically Driven Desalination. *Journal of Membrane Science* **2018,** *555*, 407-417.

46. Tang, C. Y.; She, Q.; Lay, W. C. L.; Wang, R.; Fane, A. G., Coupled Effects of Internal Concentration Polarization and Fouling on Flux Behavior of Forward Osmosis Membranes during Humic Acid Filtration. *Journal of Membrane Science* **2010,** *354*, 123-133.

47. Boo, C.; Lee, J.; Elimelech, M., Omniphobic Polyvinylidene Fluoride (PVDF) Membrane for Desalination of Shale Gas Produced Water by Membrane Distillation. *Environmental Science & Technology* **2016,** *50*, (22), 12275-12282.

48. Lu, K. J.; Zuo, J.; Chang, J.; Kuan, H. N.; Chung, T.S., Omniphobic Hollow-Fiber Membranes for Vacuum Membrane Distillation. *Environmental Science & Technology* **2018,** *52*, (7), 4472-4480.

49. Barthlott, W.; Schimmel, T.; Wiersch, S.; Koch, K.; Brede, M.; Barczewski, M.; Walheim, S.; Weis, A.; Kaltenmaier, A.; Leder, A.; Bohn, H. F., The Salvinia Paradox: Superhydrophobic Surfaces with Hydrophilic Pins for Air Retention Under Water. *Advanced Materials* **2010,** *22*, (21), 2325-2328.

50. Zhu, X.; Zhou, Y.; Hao, J.; Bao, B.; Bian, X.; Jiang, X.; Pang, J.; Zhang, H.; Jiang, Z.; Jiang, L., A Charge-Density-Tunable Three/Two-Dimensional Polymer/Graphene Oxide Heterogeneous Nanoporous Membrane for Ion Transport. *ACS Nano* **2017,** *11*, (11), 10816-10824.

51. Zhu, X.; Hao, J.; Bao, B.; Zhou, Y.; Zhang, H.; Pang, J.; Jiang, Z.; Jiang, L., Unique Ion Rectification in Hypersaline Environment: A High-Performance and Sustainable Power Generator System. *Science Advances* **2018,** *4*, (10), eaau1665.

For Table of Contents Use Only